Silver composites as highly stable cathode current collectors for solid oxide fuel cells

Ayhan Sarikaya, Vladimir Petrovsky, and Fatih Dogan[a)]
Department of Materials Science and Engineering, Missouri University of Science and Technology, Rolla, Missouri 65409

(Received 13 January 2012; accepted 4 May 2012)

Time stability of the solid oxide fuel cells (SOFCs) has been a significant concern toward realization of their practical applications. Its operation at elevated temperatures and in oxidizing atmospheres makes the cathode current collector one of the most vulnerable components of the SOFCs. Silver and silver-based metal oxide [lanthanum–strontium manganite (LSM) and yttria-stabilized zirconia] composites were investigated for the development of low-cost current collectors with long-term stability. While densification of pure silver limited its use as current collector, incorporation of oxide particles to the silver matrix led to formation of porous composites. However, addition of YSZ particles did not result in a stable porosity. Analysis of the impedance spectra allowed further investigations on the obtained microstructures and the formed contacts. No microstructural degradation has been observed in the porous Ag–LSM composite current collector and its electrical properties remained stable for over 5000 h of measurements at 800 °C in air.

I. INTRODUCTION

Ohmic losses, which arise due to the high resistance of the contact materials, have been a vital concern for the development of solid oxide fuel cells (SOFCs).[1–3] Stability and efficiency of the current collection on the cathode side of the SOFCs is a relatively more challenging issue than the anode side especially for the intermediate temperature (600–800 °C) SOFCs due to high temperature oxidation.[4–6] Common current collectors include ceramics (e.g., $LaCoO_3$ and $LaCrO_3$) and noble metals (e.g., Pt, Pd, Au, and Ag).[7] Although ceramic materials have high stability in oxidizing conditions, their lower electrical conductivities limit their use. Noble metals such as Pt, Au, or Pd are used as common current collectors stable at high temperatures, while their relatively high cost makes them less desirable for use in SOFC applications.[7–10] Its relatively low-cost and advantageous attributes such as high conductivity, high ductility, and self-healing at operating temperatures make Ag a good candidate for the current collection.[8,11] However, operational conditions deteriorate its structural stability and limit its use in SOFCs.[8,11–13] Operational temperatures of SOFCs (e.g., 800 °C) allow sintering of Ag particles and result in nearly full density of initially porous microstructure within a relatively short time (<170 h) with respect to the target lifetime of 40,000 h[14] due to relatively low melting temperature of pure Ag (962 °C), as shown in Figs. 1(a) and 1(b).[15]

Development of a porous and structurally stable Ag-based current collector was aimed by this study. Since the degradation of the cathode and anode layers limits the detailed analysis of the degradation mechanisms of the current collectors, Ag-based current collectors were applied on stable electrolytes as symmetrical electrodes to analyze their stability. Thus, the electrodes in this study should not be confused with actual anode and cathode materials of SOFCs. A systematic approach was developed to analyze the stability of the current collector compositions. The measured electrical conductivities and impedance spectra were utilized to identify the rate-limiting polarization mechanisms of the symmetrical cells. Identification of the bulk diffusion of oxygen in solid Ag as the unique polarization mechanism led to the correlation of diffusion length with the coarsening of the Ag grains and the real part of the complex polarization with the effective contact area. Porous Ag current collector was obtained by incorporating up to 25 vol% lanthanum–strontium manganite (LSM) particles while maintaining the percolation of Ag grains for sufficiently high electrical conductivity and wetting of the underlying electrolyte layer to achieve efficient current collection and stable electrical contact.

II. EXPERIMENTAL

Ag and Ag-based composite inks were prepared for screen printing of the symmetrical current collectors. Since the previous studies showed that high surface area of Ag results in structural instability,[8,16] a relatively coarse (d_{50} = 1.1 μm) Ag powder (Alfa Aesar, Ward Hill, MA)

[a)]Address all correspondence to this author.
e-mail: doganf@mst.edu
DOI: 10.1557/jmr.2012.175

 © Materials Research Society 2012

https://doi.org/10.1557/jmr.2012.175 Published online by Cambridge University Press

was used for the investigations. Initial powders of the conventional LSM–yttria-stabilized zirconia (YSZ) cathode were incorporated to the pure Ag. Utilized LSM (NexTech, Columbus, OH) and YSZ (8 mol% YSZ, TZ-8Y; TOSOH, Tokyo, Japan) powders have the average particle sizes of 0.5 μm and 25 nm, respectively. The preparation of the inks consists of the dispersion of the oxide powders (LSM or YSZ) in a solvent (α-terpineol; Alfa Aesar) by ultrasonication and mixing the dispersed suspension with Ag powder and a polymeric vehicle (V006; Hearaeus, Conshohocken, PA). The rheological properties of the inks were optimized for screen printing of symmetrical current collectors on YSZ electrolyte by adjusting the solvent and polymeric vehicle amounts. Symmetrical cells were prepared by screen printing of current collector inks on both sides of 180-μm-thick YSZ electrolyte (8 mol% YSZ; NexTech, Columbus, OH).

Electrochemical performance investigations and electrical conductivity measurements of the cells were performed using a combined potentiostat and frequency response analyzer setup (1470 CellTest; Solartron, Mobrey, UK). Four-probe electrical conductivity measurements were carried out on 0.5 × 3.0 cm rectangular samples using four Ag leads fixed perpendicular to the longer edge of the samples at certain intervals. Electrical conductivity measurements of the YSZ electrolyte were made on rectangular YSZ samples, while Ag and Ag-based composites were applied on an insulating substrate (e.g., alumina) for the conductivity measurements. Impedance measurements were carried out using two-probe configuration by fixing Ag leads on either electrode of the symmetrical cells. Impedance spectra were measured in the frequency range of 0.1 Hz to 1 MHz using an excitation voltage of 20 mV, and all electrical measurements were carried out in air to simulate the operational conditions of the cathode side of SOFCs. Scanning electron microscopy (SEM) techniques were used for the microstructural characterization of the current collectors.

III. RESULTS AND DISCUSSION

SEM micrographs shown in Fig. 1 demonstrate the microstructural development of pure Ag and Ag–20 vol% YSZ composite after measurements for various times at 800 °C. Although pure Ag reached nearly full density by closing the initially open pores in a relatively short time, Ag–20 vol% LSM composite maintained its porous microstructure without any distinguishable grain growth and coarsening over 170 h, as it was reported before.[15] Addition of the same volume of YSZ powder to the pure Ag formed initially open pores; however, the porous microstructure was not stable and Ag left the composite forming individual grains on the surface as shown in Fig. 1(d).

Although conductivity of 46,000 S/cm was measured with pure Ag at 800 °C, it showed a decreasing trend with increasing amount of LSM powder as shown in Fig. 2. As it is seen in the percolation curve, additions of LSM powder above 25 vol% would lower the conductivity below the target limit of the electrical conductivity, which was 100 S/cm for this study. Thus, the Ag–25 vol% LSM composition was analyzed as the highly loaded composite mixture to investigate the stability of Ag–LSM current collectors.

Ag–25 vol% LSM composite maintained its initially open porosity and microstructural stability after 170 h of continuous electrochemical measurements simulating its operational conditions, as shown in Fig. 3. The microstructure of Ag–25 vol% LSM was similar to the microstructure of Ag–20 vol% LSM observed by the authors previously.[17]

Although electrical conductivity of the Ag–25 vol% LSM composite current collector was sufficiently high, its performance by forming an efficient contact with the underlying layer was crucial for the current collection in operational SOFC configurations. The analysis of the obtained impedance spectra was utilized for further investigations

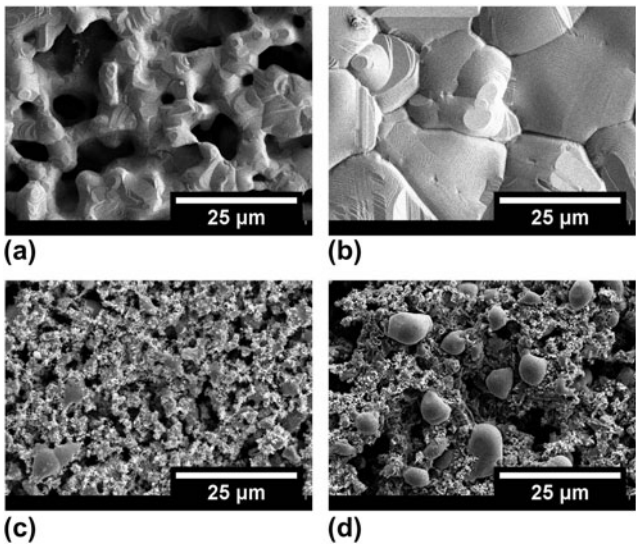


FIG. 1. SEM micrographs of (a, b) pure Ag[15] and (c, d) Ag–20 vol% YSZ, both obtained after 2 and 170 h of measurements at 800 °C, respectively.

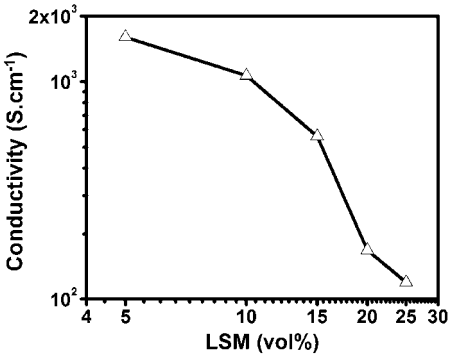


FIG. 2. Electrical conductivity of Ag composites with various LSM loadings at 800 °C in air.

https://doi.org/10.1557/jmr.2012.175 Published online by Cambridge University Press

of the contact interface between the current collector and the electrolyte.

Impedance spectra consist of ohmic and polarization resistances. Since ohmic resistance of symmetrical cells can be obtained from the high frequency x-axis intercepts of Cole–Cole plots,[17] ohmic and polarization resistances can be distinguished in the impedance spectra. The measured ohmic resistance involves the electrical resistances of symmetrical current collectors and the electrolyte. However, impedance spectroscopy is not capable of differentiating the contributing ohmic components. Therefore, the resistance of the electrolyte was required to be excluded from the obtained ohmic resistance to determine the resistance of the current collector accurately. The electrical resistance of the YSZ electrolyte was measured by four-probe electrical conductivity measurement technique and an area-specific ohmic resistance (ASR) of 0.25 Ωcm^2 was calculated for 180-μm-thick electrolytes at 800 °C. Since YSZ electrolyte, symmetrical pure Ag cell, and symmetrical Ag–25 vol% LSM cell demonstrated the same ASR of 0.25 Ωcm^2 as shown in Fig. 4, it can be concluded that the contact resistance was stable and negligible for both Ag-based current collectors.

Further analysis of the impedance data by complex nonlinear least square fitting to equivalent circuit models revealed that the impedance spectra could be interpreted using an equivalent circuit, which consists of a resistor and a finite-length Warburg element with transmissive boundary conditions in series as shown in Fig. 5. It is in good agreement with the configuration of the symmetrical cell since the proposed Warburg element represents the diffusion of charged particles to a planar electrolyte.[18]

The Warburg impedance which is attributed to finite-length diffusion with transmissive boundary conditions is described by Eq. (1):

$$W = R_w \frac{\tanh\sqrt{j\omega\tau_w}}{\sqrt{j\omega\tau_w}} \quad , \qquad (1)$$

where R_w is the Warburg polarization resistance and τ_w is the time constant.

The characteristic relaxation frequency of the corresponding Warburg polarization mechanism can be calculated using the following equation and correlated with the mean diffusion time of oxygen, τ, obtained from the fitting:

$$f_w = \frac{1}{(2\pi\tau_w)} \quad . \qquad (2)$$

Although a good fit of the measured impedance spectra to the finite-length Warburg element with less than 1% deviation suggests that the observed polarization mechanism is dictated by diffusion, the nature of the diffusion was required to be identified for further analysis of the current collectors. Therefore, the characteristic relaxation frequencies were obtained from the fitting of the impedance spectra measured at various temperatures. Analysis of the temperature dependence of the characteristic relaxation frequency allowed determination of the activation energy for the dominating diffusion mechanism.[19,20]

The solubility and mobility of oxygen within the bulk solid Ag have been studied by other researchers.[21–25] Their investigations revealed that oxygen has high solubility and mobility in solid Ag. The activation energy for the dominating polarization mechanism, calculated from the temperature dependence of the characteristic relaxation frequency, was in a good agreement with their results and revealed that the rate-determining mechanism was the diffusion of oxygen atoms through bulk Ag as shown in Fig. 6. Although the decreasing porosity of pure Ag could

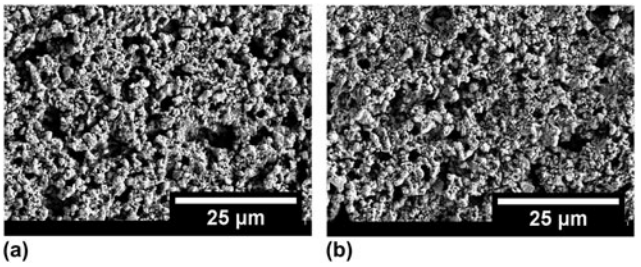


FIG. 3. SEM micrographs of (a, b) Ag–25 vol% LSM obtained after 2 and 170 h of measurements at 800 °C, respectively.

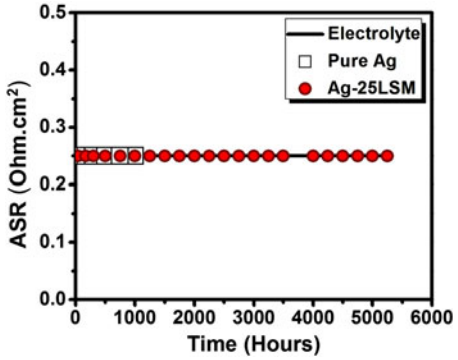


FIG. 4. Area-specific resistances of the YSZ electrolyte, symmetrical pure Ag cell, and symmetrical Ag–25 vol% LSM cell at 800 °C as a function of time.

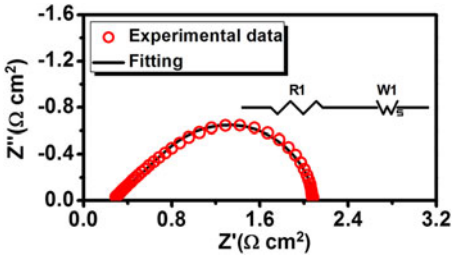


FIG. 5. Cole–Cole plot of the experimental data of pure Ag measured at 800 °C and its fitting according to the equivalent circuit model.

https://doi.org/10.1557/jmr.2012.175 Published online by Cambridge University Press

also give rise to the limitation of the transport of gases, relatively low activation energies should have been observed if the polarization was induced by the gas phase diffusion.[26] Therefore, it suggests that the bulk diffusion is the controlling transport mechanism for oxygen in solid Ag.

Thus, the following equation was used for the diffusion coefficient, $D_{O,Ag(S)}$, with reasonable accuracy[23]:

$$D_{O,Ag(S)} = 4.9 \times 10^{-3} \exp\left(\frac{-0.503\,\text{eV}}{RT}\right) \quad . \qquad (3)$$

Since the characteristic relaxation frequency, f_w, is not dependent on the surface area in the symmetrical cell configuration, the diffusion length of oxygen as charge carrier can be calculated according to the following equation[27]:

$$L_d = \sqrt{D\tau_w} = \sqrt{\frac{D}{2\pi f_w}} \quad . \qquad (4)$$

Results of the impedance spectroscopy measurements on the symmetrical cell with pure Ag revealed that the relaxation frequency corresponding to the electrode polarization decreases with time as shown in Fig. 7(a). Diffusion length, L_d, was associated with the characteristic relaxation frequency using the diffusion constant, $D_{O,Ag(S)}$, at the measurement temperature (800 °C) by using Eq. (4). Densification of initially porous Ag is reflected in the change of diffusion length, which is correlated with the relaxation frequencies obtained from the fitting of impedance spectra. The shift to the lower relaxation frequencies is attributed to longer diffusion length of oxygen through larger grains of dense solid Ag as compared to shorter diffusion length of oxygen through smaller grains of initially porous Ag, as shown in Fig. 7(b). Calculated diffusion lengths are in good agreement with the grain sizes observed in the analysis of the densifying microstructure of pure Ag, as shown in Figs. 1(a)–1(b). The thickness of the dense pure Ag current collector on the YSZ electrolyte was measured after 600 h of measurements at 800 °C. Its measured thickness of ~38 μm showed a good agreement with the calculated diffusion length of 43.4 μm.

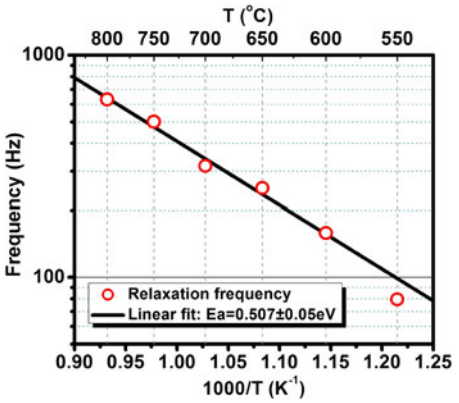


FIG. 6. Temperature dependence of the characteristic relaxation frequency of Warburg impedance.

The electrical resistance of a current collector is formulated by the following equation:

$$R = \frac{1}{\sigma} \times \frac{L}{A} \quad . \qquad (5)$$

The electrode polarization due to the diffusion of oxygen through bulk Ag resulted in the complex impedance, expressed by the Warburg element. The real part of this complex impedance can be resolved as Warburg resistance, R_w. Thus, it would yield an ASR normalized to the surface area of the symmetrical current collector. In this case, the conductivity component, σ, of the Eq. (5), can be described as the conductivity due to the diffusion of oxygen through solid Ag, and the length component (L) can be interpreted as the diffusion length (L_d) that is expressed by the following equation:

$$\text{ASR} = \frac{1}{\sigma} \times L_d \quad . \qquad (6)$$

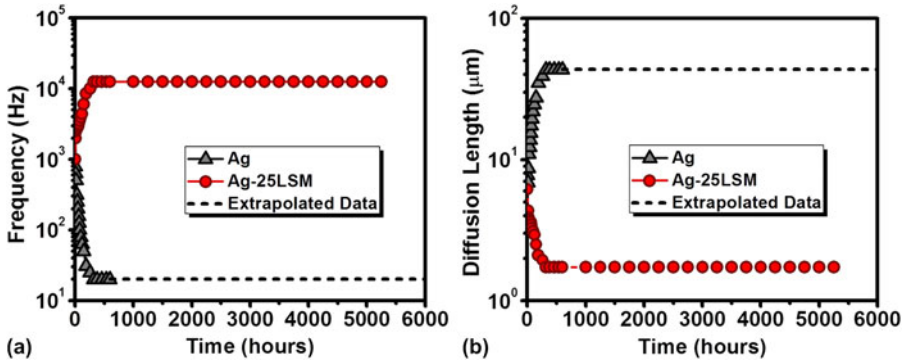


FIG. 7. (a) Characteristic relaxation frequency and (b) diffusion length as functions of time calculated from the impedance spectra of the pure Ag and Ag–25 vol% LSM cells measured at 800 °C.

https://doi.org/10.1557/jmr.2012.175 Published online by Cambridge University Press

The normalized surface area of the current collector could be assumed completely covered with a fully dense pure Ag upon densification and saturation of the diffusion length after 600 h at 800 °C in air as shown in Fig. 7. However, Ag–25 vol% LSM was not capable of providing the same coverage of the contact surface due to its porous microstructure. Thus, a coverage coefficient, α, was introduced to the Eq. (6) where it reaches to the unity in the case of the total coverage of the electrolyte surface area with dense Ag as formulated by the following equation:

$$\mathrm{ASR} = \frac{1}{\sigma} \times \frac{L_\mathrm{d}}{\alpha} \quad . \tag{7}$$

The polarization resistance of pure Ag current collector demonstrated an increasing trend with time, while the Ag–25 vol% LSM current collector exhibited a decreasing polarization resistance; however, the polarization resistances of both Ag-based current collectors stabilized after around 300 h of measurements at 800 °C. Since the conductivity due to the diffusion of oxygen atoms through solid Ag, σ, is constant for all Ag-based current collectors, effective contact area can be estimated using the coverage coefficient, α, calculated using the measured ASRs and determined diffusion lengths. Therefore, the coverage coefficients of both Ag and Ag–25 vol% LSM current collectors increased with time and reached to stable values during the measurements at 800 °C, as shown in Fig. 8. This suggests that the Ag–25 vol% LSM composite current collector developed a better contact with the underlying electrolyte with time and covered 1.5% ($\alpha = 0.015$) of the available surface area, while pure Ag also developed a better contact with increasing time and covered 100% ($\alpha = 1$) of the available surface area approximately within the same time period.

Since the samples were not exposed to elevated temperatures prior to the measurements, microstructural changes (e.g., densification and coarsening) took place as they were heated up to the measurement temperatures (e.g., 800 °C). As the connectivity between Ag grains and their contact with the YSZ electrolyte were developed, oxygen atoms were transferred through shorter diffusion lengths. These initial microstructural changes in Ag–25 vol% LSM composite current collector resulted in an increase in the measured characteristic relaxation frequency, which stabilized after ~300 h. The initial increase and the saturation in the characteristic relaxation frequency are attributed to a decrease in the diffusion length followed by the stabilization of the obtained porous microstructure as shown in Fig. 7(b). On the other hand, the symmetrical cell of pure Ag exhibited a decrease in the characteristic relaxation frequency with time during the initial stage of the measurements (~300 h), which can be interpreted as the coarsening of Ag grains and further densification of bulk Ag. There were no further changes in the characteristic relaxation frequency for the rest of the measurements (>4700 h). The densification of the Ag on the electrolyte surface led to the coverage of the total available contact area. Thus, the identified coverage coefficient, α, reached to the unity with time and a good contact was maintained during the measurements as shown in Fig. 8. In the case of Ag–25 vol% LSM composite current collector, α showed a significant increase over a period of time (~300 h) but could not reach the unity and stabilized at 0.015. The fact that there is no degradation in the smaller contact area obtained by incorporation of LSM particles into Ag confirms the observed stable porous microstructure of the Ag–25 vol% LSM current collector shown in Figs. 3(a) and 3(b).

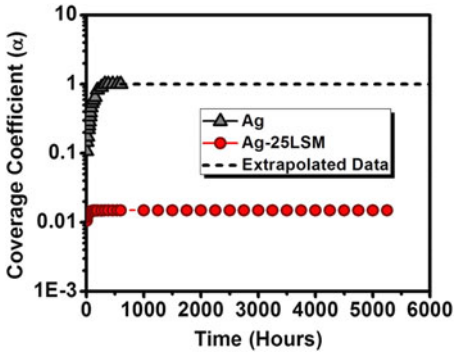


FIG. 8. Change of the effective contact area represented by the calculated coverage coefficient, α, with increasing time at 800 °C.

Although densification of Ag was hindered by the uniformly dispersed LSM particles inhibiting the grain growth, percolation of Ag grains was maintained by neck formation between Ag particles and conductive nature of Ag matrix remained unaffected by addition of LSM. A stable contact was formed at the electrolyte interface without coarsening of Ag grains or delamination of the composite electrode, although the Ag matrix contained a relatively high amount of LSM particles (25 vol%). Ag–LSM composite current collector showed no ohmic loss and a stable contact for a significantly long period of time without any microstructural changes. The use of Ag–LSM current collector and Cr blocking feature of LSM may also realize the use of relatively inexpensive Cr containing ferritic steel as interconnect material to build SOFC stacks.[7]

IV. CONCLUSIONS

Analysis of the microstructures using SEM and electrical measurements of symmetrical cells by impedance spectroscopy demonstrated that highly stable silver-based current collectors were obtained for cathodes of SOFCs by incorporation of LSM particles into the Ag matrix. Addition of LSM terminated the densification of Ag particles and led to a stable porous microstructure of the composite current collector, while the ohmic resistance remained unchanged after >5000 h of measurements at 800 °C in air. Further

https://doi.org/10.1557/jmr.2012.175 Published online by Cambridge University Press

studies will focus on the evaluation of Ag–LSM current collectors on symmetrical cathode layers, complete fuel cells, and stacks.

ACKNOWLEDGMENTS

This work was supported by a grant of the AFRL under Contract No. FA4819-09-C-0018. Utilization of SEM facilities at the Graduate Center for Materials Research (MRC) of Missouri S&T is greatly acknowledged.

REFERENCES

1. W. Schafer, A. Koch, U. Herold-Schmidt, and D. Stolten: Materials, interfaces and production techniques for planar solid oxide fuel cells. *Solid State Ionics* **86–88**, 1235 (1996).
2. S. Koch and P.V. Hendriksen: Contact resistance at ceramic interfaces and its dependence on mechanical load. *Solid State Ionics* **168**, 1 (2004).
3. X.D. Zhou, L.R. Pederson, J.W. Templeton, and J.W. Stevenson: Electrochemical performance and stability of the cathode for solid oxide fuel cells. *J. Electrochem. Soc.* **157**, B220 (2010).
4. K. Huang, P.Y. Hou, and J.B. Goodenough: Characterization of iron-based alloy interconnects for reduced temperature solid oxide fuel cells. *Solid State Ionics* **129**, 237 (2000).
5. J. Piron-Abellan, V. Shemet, F. Tietz, L. Singheiser, and W.J. Quadakkers: Ferritic steel interconnect for reduced temperature SOFC, in *Proceedings of the Seventh International Symposium on Solid Oxide Fuel Cells*; H. Yokokawa and S.C. Singhal, eds., PV 2001-16, The Electrochemical Proceedings Series, Pennington, NJ, 2001; p. 811.
6. Z. Yang, K.S. Weil, D.M. Paxton, and J.W. Stevenson: Selection and evaluation of heat-resistant alloys for SOFC interconnect applications. *J. Electrochem. Soc.* **150**, A1188 (2003).
7. L.T. Wilkinson and J.H. Zhu: Ag-perovskite composite materials for SOFC cathode–interconnect contact. *J. Electrochem. Soc.* **156**, B905–B912 (2009).
8. Z. Yang, G. Xia, P. Singh, and J.W. Stevenson: Electrical contacts between cathodes and metallic interconnects in solid oxide fuel cells. *J. Power Sources* **155**, 246 (2006).
9. S.P. Simner, M.D. Anderson, J.E. Coleman, and J.W. Stevenson: Performance of a novel La(Sr)Fe(Co)O_3–Ag SOFC cathode. *J. Power Sources* **161**, 115 (2006).
10. S.P. Simner, M.D. Anderson, L.R. Pederson, and J.W. Stevenson: Performance variability of La(Sr)FeO_3 SOFC cathode with Pt, Ag, and Au current collectors. *J. Electrochem. Soc.* **152**, A1851 (2005).
11. T.B. Sheppard and B.S.J. Kang: Development of candidate silver Cermet contact materials for cathode side in solid oxide fuel cell, in *Proceedings of Materials Science and Technology Conference (MS&T) 2007*, P. Singh, A-M. Azad, D.C. Collins, P.N. Kumta, C. Legzdins, A. Manthiram, A. Manicannan, S.K. Sundaram and Z.G. Yang, eds., PV 2007-2, Detroit, MI, 2007; p. 1209.
12. P. Singh, Z. Yang, V. Viswanathan, and J.W. Stevenson: Observations on the structural degradation of silver during simultaneous exposure to oxidizing and reducing environments. *J. Mater. Eng. Perform.* **13**, 287 (2004).
13. M. Camaratta and E.D. Wachsman: Silver-bismuth oxide cathodes for IT-SOFCs; Part I-microstructural instability. *Solid State Ionics* **178**, 1242 (2007).
14. H.U. Anderson and F. Tietz: Interconnects, in *High Temperature Solid Oxide Fuel Cells: Fundamentals, Design and Applications*, edited by S.C. Singhal and K. Kendall (Elsevier Advanced Technology, Oxford, UK, 2003) p. 183.
15. A. Sarikaya, V. Petrovsky, and F. Dogan: Development of a silver based current collector for SOFC cathodes, in *In-Situ Studies of Solid-Oxide Fuel-Cell Materials*, edited by R. Maher (Mater. Res. Soc. Symp. Proc. **1385**, Warrendale, PA, 2012) MRSF11-1385-C07-10.
16. W.A. Meulenberg, O. Teller, U. Flesch, H.P. Buchkremer, and D. Stöver: Improved contacting by the use of silver in solid oxide fuel cells up to an operating temperature of 800 °C. *J. Mater. Sci.* **36**, 3189 (2001).
17. Z. Wang, N. Zhang, J. Qiao, K. Sun, and P. Xu: Improved SOFC performance with continuously graded anode functional layer. *Electrochem. Commun.* **11**, 1120 (2009).
18. E. Barsoukov and J.R. Macdonald: *Impedance Spectroscopy: Theory, Experiment, and Applications* (John Wiley & Sons, Inc., Hoboken, NJ, 2005) p. 84.
19. S. Lanfredi and A.C.M. Rodrigues: Impedance spectroscopy study of the electrical conductivity and dielectric constant of polycrystalline $LiNbO_3$. *J. Appl. Phys.* **86**, 2215 (1999).
20. P. Jasinski, V. Petrovsky, T. Suzuki, and H.U. Anderson: Impedance studies of diffusion phenomena and ionic and electronic conductivity of cerium oxide. *J. Electrochem. Soc.* **152**, J27 (2005).
21. H. Möbius and B. Rohland: Oxygen-ion-conducting solid electrolytes and their applications. XIV. Effect of the electrode material on the results of electrical conductivity measurements in solid electrolytes. *Z. Chem.* **6**, 158 (1966).
22. S. Badwal, M. Bannister, and M. Murray: Non-stoichiometric oxide electrodes for solid state electrochemical devices. *J. Electroanal. Chem.* **168**, 363 (1984).
23. T.A. Ramanarayanan and R.A. Rapp: The diffusivity and solubility of oxygen in liquid tin and solid silver and the diffusivity. *Metall. Mater. Trans. B* **3**, 3239 (1972).
24. I. Kontoulis and B.C.H. Steele: Determination of oxygen diffusion in solid Ag by an electrochemical technique. *Solid State Ionics* **47**, 317 (1991).
25. JH. Park: Measuring oxygen diffusivity and solubility in solid silver with a gas-tight electrochemical cell. *Mater. Lett.* **9**, 313 (1990).
26. M. Kanezashi, J. O'Brien-Abraham, Y.S. Lin, and K. Suzuki: Gas permeation through DDR-type zeolite membranes at high temperatures. *AlChE J.* **54**, 1478 (2008).
27. C.T. Sah: *Fundamentals of Solid-State Electronics* (World Scientific Publishing, Singapore, 1991) p. 436.

https://doi.org/10.1557/jmr.2012.175 Published online by Cambridge University Press